Journal of Power Sources 296 (2015) 204–214

Contents lists available at ScienceDirect

Journal of Power Sources

journal homepage: www.elsevier.com/locate/jpowsour

Polybenzimidazole-crosslinked poly(vinylbenzyl chloride) with quaternary 1,4-diazabicyclo (2.2.2) octane groups as high-performance anion exchange membrane for fuel cells

Wangting Lu [a, b], Geng Zhang [c, b], Jin Li [b], Jinkai Hao [b, d], Feng Wei [a], Wenhui Li [a], Jiying Zhang [a], Zhi-Gang Shao [b, *], Baolian Yi [b]

[a] Institute for Interdisciplinary Research, Jianghan University, 430056, Wuhan, PR China
[b] Fuel Cell System and Engineering Research Group, Dalian Institute of Chemical Physics, Chinese Academy of Sciences, 457 Zhongshan Road, Dalian, 116023, PR China
[c] Department of Chemistry, College of Science, Huazhong Agricultural University, 430070, Wuhan, PR China
[d] University of Chinese Academy of Sciences, 19A Yuquan Road, Beijing, 100049, PR China

HIGHLIGHTS

- A uniform, compact and tough AEM is prepared by crosslinking between PBI and PVBC.
- Two kinds of crosslinking points are identified in the crosslinked AEM.
- DABCO is used as the quaternization reagent and only one nitrogen atom is converted.
- The AEM presents high ionic conductivity, low swelling and superior stability.
- The fuel cell using AEM herein shows high power output and durability.

GRAPHICAL ABSTRACT

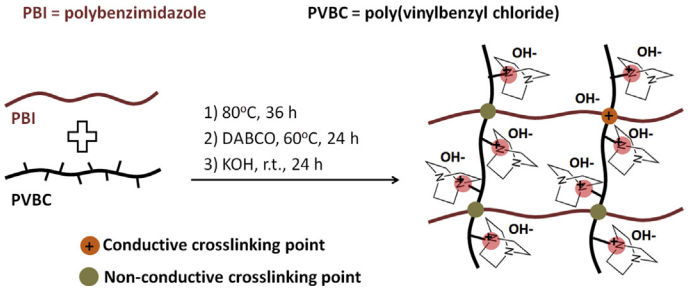

ARTICLE INFO

Article history:
Received 1 April 2015
Received in revised form
1 July 2015
Accepted 15 July 2015
Available online 25 July 2015

Keywords:
Anion exchange membrane fuel cell
Crosslinked membrane
Polybenzimidazole
1,4-diazabicyclo (2.2.2) octane
Stability

ABSTRACT

Development of anion exchange membrane (AEM) with high conductivity, good dimensional stability, desirable toughness and long life-time simultaneously is still a challenge for the practical application of AEM fuel cells. Herein, a novel AEM (denoted as PBI-c-PVBC/OH) is fabricated by applying polybenzimidazole (PBI) and 1,4-diazabicyclo (2.2.2) octane (DABCO) as the macromolecular crosslinker and quaternizing reagent for poly(vinylbenzyl chloride) (PVBC), respectively. With the aid of crosslinking by PBI, PBI-c-PVBC/OH exhibits good flexibility and strength both in dry and water-saturated state. Moreover, high hydroxide conductivity (>25 mS cm^{-1} at room temperature) and low swelling ratio (~13%) is obtained, especially the swelling ratio nearly does not increase with temperature. The membrane is also advanced for the superior chemical stability in alkaline environment due to the stable polymer backbone and ionic conductive group (only one nitrogen atom in a DABCO molecule is quaternized). Furthermore, a peak power density of 230 mW cm^{-2} at 50 °C is obtained on the H_2/O_2 fuel cell using PBI-c-PVBC/OH, and the membrane presents high durability both in the constant current and continuous open circuit voltage testing. Therefore, it is considered that the PBI crosslinking together with DABCO quaternization can be regarded as a promising strategy in the development of AEM for fuel cells.

* Corresponding author.
E-mail address: zhgshao@dicp.ac.cn (Z.-G. Shao).

http://dx.doi.org/10.1016/j.jpowsour.2015.07.048
0378-7753/

1. Introduction

Anion exchange membrane fuel cell (AEMFC) working under alkaline conditions has many advantages compared with its counterpart, proton exchange membrane fuel cell, such as faster electrode kinetics, lower alcohol crossover and non-noble metal electrocatalysts [1–3]. In an AEMFC, anion exchange membrane (AEM) is a crucial component, which plays the role as transporting OH^- and preventing the mix between oxygen/air and fuel. AEMs are generally made up of polymer matrix and anion exchange groups. The polymer matrix is usually hydrophobic and it is used to support the whole membrane, while anion exchange groups are hydrophilic and they can be dissociated into fixed cationic head groups and free hydroxide after absorbing water, giving the ion transporting ability to AEM. As a polymer electrolyte membrane, high ionic conductivity is always admired, which usually requires large quantity of ion exchange groups in the membrane, especially for the AEM, because the mobility of OH^- is only ~57% that of H^+ in aqueous phase [3]. Nevertheless, more anion exchange groups means more water will be absorbed by the AEM, resulting in severe swelling and poor strength [1–5]. Several strategies have been put forward to attempt to resolve this problem, such as crosslinking [6–9] and self-aggregation strategy [10–13]. However, it is still a challenge to obtain AEM with desirable conductivity, dimensional stability and toughness simultaneously. There are reasons to believe that fabricating an AEM consisting of two components with mechanical-supporting and hydroxide-conducting function, respectively, perhaps better overcomes the difficulty. Thus, composite AEM [14,15] and semi-interpenetrated polymer network (semi-IPN) [16,17] were developed, which are usually formed by combining a hydroxide-conducting polymer with a supporting polymer having high thermal, mechanical and chemical stabilities. Nevertheless, the separation of two components would occur in the semi-IPN or composite membrane due to the obvious differences in properties and the weak interaction between them, which often results in poor performances [18,19].

In addition to the aforementioned dilemma, another challenge faced by AEM is the degradation of polymer backbone (*e.g.*, aromatic-ether structure) and anion exchange group (*e.g.*, quaternary ammonium) following Hofmann Elimination or nucleophilic substitution by OH^- [1,4]. Constructing more stable polymer structure and adopting alkaline-resistant cationic head group are believed to be effective solutions to this troublesome problem [20–24]. For example, benzyltrimethylammonium quaternary ammonium (QA) is the most commonly used ionic conductive group in AEMs, but its chemical stability under alkaline environment needs to be enhanced [3]. Subsequently, it was found that the QA group converted from 1,4-diazabicyclo (2.2.2) octane (DABCO) with only one nitrogen group reacted was highly alkaline resistant due to its rigid cage structure despite that β-hydrogen atoms existed in this group [2,3]. However, it was difficult to produce AEM with such structure, because both of the two nitrogen atoms in DABCO tended to react, forming crosslink [25–28]. Unfortunately, the DABCO-formed crosslinks will give rise to materials with low alkaline stability [2,3].

In the present work, a novel AEM was prepared based on polybenzimidazole (PBI) and poly(vinylbenzyl chloride) (PVBC), in which the tough and alkaline-resistant PBI was adopted as the mechanical-supporting component, while 1, 4-diazabicyclo (2.2.2) octane (DABCO) partially quaternized PVBC took charge of conducting hydroxide. In this AEM, crosslinking was formed between two polymers *via* the reaction of chloromethyl groups of PVBC with benzimidazole groups of PBI, thus the interaction between the two different components was strong and the component separation was avoided, producing a uniform distribution of ionic conductive groups in the AEM [29]. Moreover, thanks to the crosslinking with PBI, excess swelling of AEM by water was suppressed, and the mechanical properties of PVBC were improved. The ionic conductive group was introduced by quaternizing the remaining chloromethyl groups of PVBC with DABCO, and the novelty was that only one nitrogen atom of the DABCO molecule was reacted, *i.e.*, the "selective conversion of DABCO" (*i.e.*, only one nitrogen in a DABCO molecule was quaternized) was realized. The high stability of cationic head groups obtained was eventually confirmed by experiments. In addition, the AEM here was fabricated without chloromethylation reaction, which was restricted because of the application of highly carcinogenic reagent (*e.g.*, chloromethyl methyl ether) and the difficulty of precise controlling the location and degree of chloromethylation [30].

2. Experimental section

2.1. Materials

Polybenzimidazole (PBI, $M_w = 9.6 \times 10^4$ g mol^{-1} measured by viscometric method using Ubbelohde viscometer) was synthesized in our lab and its nuclear magnetic resonance (NMR) spectrum (Fig. S1) and Fourier transform infrared (FT-IR) absorption spectrum (Fig. S2) was in good agreement with those shown in literature [31]. 1, 4-diazabicyclo (2.2.2) octane (DABCO) and poly(vinylbenzyl chloride) (PVBC, 60/40 mixture of 3- and 4-isomers average M_n ~ 55,000, average M_w ~ 100,000 by GPC/MALLS, powder) were procured from Sigma–Aldrich. Benzimidazole (BIm) and benzyl chloride (BC) came from Aladdin (China) and J&K Chemical, respectively. The electrocatalyst used in the fuel cell testing was 70 wt.% Pt/C (Johnson Matthey) and the ionomer was AS-4 ionomer (Tokuyama Co., Japan). The polymer concentration of AS-4 is 5 wt.% with 1-propanol as the solvent; the polymer has linear hydrocarbon backbone with quaternary ammonium group; the ion exchange capacity of the polymer is 1.3 mmol g^{-1} and the HCO_3^- conductivity is 13 mS cm^{-1} at 40 °C (http://www1.eere.energy.gov/hydrogenandfuelcells/pdfs/amfc_050811_fukuta.pdf). All other chemicals used were commercially available with analytical grade. Moreover, all chemicals were used without further treatment.

2.2. Preparation of PBI-c-PVBC/OH membrane

Typically, a PBI and PVBC mixed solution was prepared by dissolving 0.15 g PBI in N-methyl-2-pyrrolidone (NMP) followed by adding 0.15 g PVBC. After complete dissolution, the mixed polymer solution was casted on a glass plate, and dried in an oven at 80 °C. A petri dish was covered on the top of the casting solution to slow down the evaporation rate of solvent. After 24 h, the petri dish was taken away and the membrane was heated for another 12 h to remove the solvent completely, obtaining a membrane denoted as PBI-c-PVBC. Subsequently, the PBI-c-PVBC membrane was quaternized by soaking in 0.5 mol L^{-1} DABCO ethanol solution for 24 h at 60 °C, giving rise to a Cl^- form AEM, named as PBI-c-PVBC/Cl. Next, PBI-c-PVBC/Cl was converted to the OH^- form membrane (PBI-c-PVBC/OH) by immersing PBI-c-PVBC/Cl in a 1 mol L^{-1} KOH aqueous solution for 24 h. In order to remove residual KOH from PBI-c-PVBC/OH, the membrane was washed by ultrapure water repeatedly and sealed in ultrapure water for 36 h.

2.3. Model reaction

In order to investigate the structure of reaction product between PBI and PVBC, a model reaction was performed using BIm and BC under similar reacting conditions with that of PBI-c-PVBC

membrane. Briefly, 57.5 mg (0.487 mmol) BIm and 124.5 mg (0.984 mmol) BC was added into 4.5 mL NMP, in which the concentration of benzimidazole group and chloromethyl group was the same with that of repeating unit of PBI and PVBC in the membrane casting solution, respectively. The above solution was sealed and heated at 80 °C for 5 h, and then dried at 80 °C for another 36 h to obtain the product.

2.4. Structure characterization

The FT-IR absorption spectra of membranes were recorded on a Bruker Tensor 27 spectrophotometer. ^{1}H NMR spectra were obtained on a NMR spectrometer (Bruker Avance II 400) at 400.13 MHz using DMSO-d_6 as the solvent with tetramethylsilane as the internal standard. The morphology of membrane was observed on a JEOL JSM-6360LV scanning electron microscope (SEM). The elemental analysis of membrane was conducted by Oxford Inca EDX detector equipped on FEI Quanta 450 SEM and Hitachi S4800 SEM. The thermal stability of membrane was tested on a Mettler Toledo TGA/SDTA851 analyzer from room temperature to 700 °C at a heating rate of 10 °C min^{-1} under N_2 flow. The X-ray photoelectron spectrum (XPS) of membrane was recorded on a Thermo Scientific ESCALAB 250Xi spectrometer with Al K_α radiation. The stress versus strain curve of membrane was recorded on a universal testing machine (Changchun KeXin Corporation, China). The crystalline structure of membrane was examined by an X-ray diffractometer (XRD, Bruker D8 ADVANCE) with Cu K_α radiation.

2.5. Ion exchange capacity, swelling ratio, water uptake and ionic conductivity

The ion exchange capacity (IEC) of membrane was measured by a back titration method: the vacuum-dried OH^- form membrane was immersed in 0.01 mol L^{-1} HCl solution (20 mL) for 24 h, and then the solution was back titrated using 0.01 mol L^{-1} NaOH solution in the presence of an indicator (phenolphthalein). A 0.01 mol L^{-1} HCl solution (20 mL) was titrated as the blank sample. The IEC (mmol g^{-1}) of the membrane can be calculated as follows:

$$\mathrm{IEC} = (V_b - V_a)c_{HCl} \Big/ m_{dry} \quad (1)$$

where m_{dry} was the mass of dry membrane; c_{HCl} was the concentration of HCl solution; V_a and V_b was the consumed volume of the NaOH solution for the test sample and blank sample, respectively.

The water uptake (WU) and swelling ratio (SR) of membrane were calculated by equations:

$$\mathrm{WU} = \left(m_{wet} - m_{dry}\right) \Big/ m_{dry} \quad (2)$$

$$\mathrm{SR} = \left(l_{wet} - l_{dry}\right) \Big/ l_{dry} \quad (3)$$

where m_{wet} and l_{wet} was the mass and average length of wet membrane, respectively, in which $l_{wet} = (a_{wet} \cdot b_{wet})^{1/2}$, a_{wet} and b_{wet} was the length and width of wet membrane sample, respectively; m_{dry} and l_{dry} was the mass and average length of dry membrane, respectively, in which $l_{dry} = (a_{dry} \cdot b_{dry})^{1/2}$, a_{dry} and b_{dry} was the length and width of dry membrane sample, respectively.

A two-probe AC impedance method was applied to measure the ionic conductivity of membrane by using a Solartron 1260 & 1287 electrochemical workstation under the potentiostatic mode. The measurement was conducted in a frequency between 1 MHz and 1 Hz with an AC potential of 10 mV. In order to minimize the interference by ambient CO_2, the OH^- form AEM was taken out from the sealed container filled with ultrapure water when measurement was performed, and then set up in the testing fixture (shown in Fig. S3). The fixture was submerged in a beaker filled with ultrapure water and the beaker was placed in a thermostatic chamber. The water in the beaker was refreshed after every measurement. The ionic conductivity of the membrane, σ (mS cm^{-1}), was calculated by:

$$\sigma = l/wdR \quad (4)$$

where R was the membrane resistance (kΩ); d and w was the cross-sectional thickness and width (cm) of the membrane, respectively; l was the length of the sample (cm) between two electrodes.

2.6. Gel fraction measurement

A piece of PBI-c-PVBC membrane was weighed and immersed in NMP at 80 °C. After certain periods of time, the membrane was collected, washed with ultrapure water, dried and weighed. The ratio of the residual mass was identified as the gel fraction, which can be used to evaluate the crosslinking density of the membrane.

2.7. Alkaline and oxidative stability

The stability of PBI-c-PVBC/OH membrane in alkaline environment was evaluated by immersing the membrane in 1 mol L^{-1} KOH at 60 °C. The hydroxide conductivity of the sample was measured at room temperature by the aforementioned method after a certain time. The oxidative stability of PBI-c-PVBC/OH membrane was assessed by soaking the membrane in Fenton's reagent (4×10^{-6} mol L^{-1} $FeSO_4$ in 3% H_2O_2) at 40 °C. The weight of the membrane sample was measured on an electronic balance after absorbing the superficial liquid with filter paper at a certain time interval.

2.8. Single fuel cell testing

The performances of PBI-c-PVBC/OH membrane were further evaluated in a single AEMFC. In this work, gas diffusion electrodes (GDE) fabricated by commercially available gas diffusion layer, Pt/C catalysts and AS-4 ionomer were adopted in the single cell testing. The detailed preparation procedures of GDE and membrane electrode assembly (MEA), as well as the performing conditions of the fuel cell, can be obtained in our previous work [29].

A constant current testing (100 mA cm^{-2}) was conducted to evaluate the stability of the fuel cell, during which the fuel cell voltage was monitored. Electrochemical impedance spectra (EIS) of the fuel cell before and after constant current testing were recorded by a Kikusui KFM-2030 impedance meter under the galvanostatic mode (100 mA cm^{-2}) with a frequency range between 10 kHz and 1 Hz. Additionally, the oxidative stability of PBI-c-PVBC/OH was assessed under continuous open circuit voltage (OCV) conditions, during which the hydrogen crossover current of the fuel cell was measured at intervals according to the literature [32].

3. Results and discussion

3.1. Structure analysis of PBI-c-PVBC membrane

The preparation pathway of AEM was illustrated in Fig. 1. First of all, PBI and PVBC were dissolved in NMP successively, and then the mixture was casted and dried at 80 °C; the membrane obtained in this step was named as PBI-c-PVBC. As displayed in Fig. S4, PBI-c-PVBC was transparent and homogeneous, similar with PBI in appearance. The PBI-c-PVBC membrane presented FT-IR adsorption

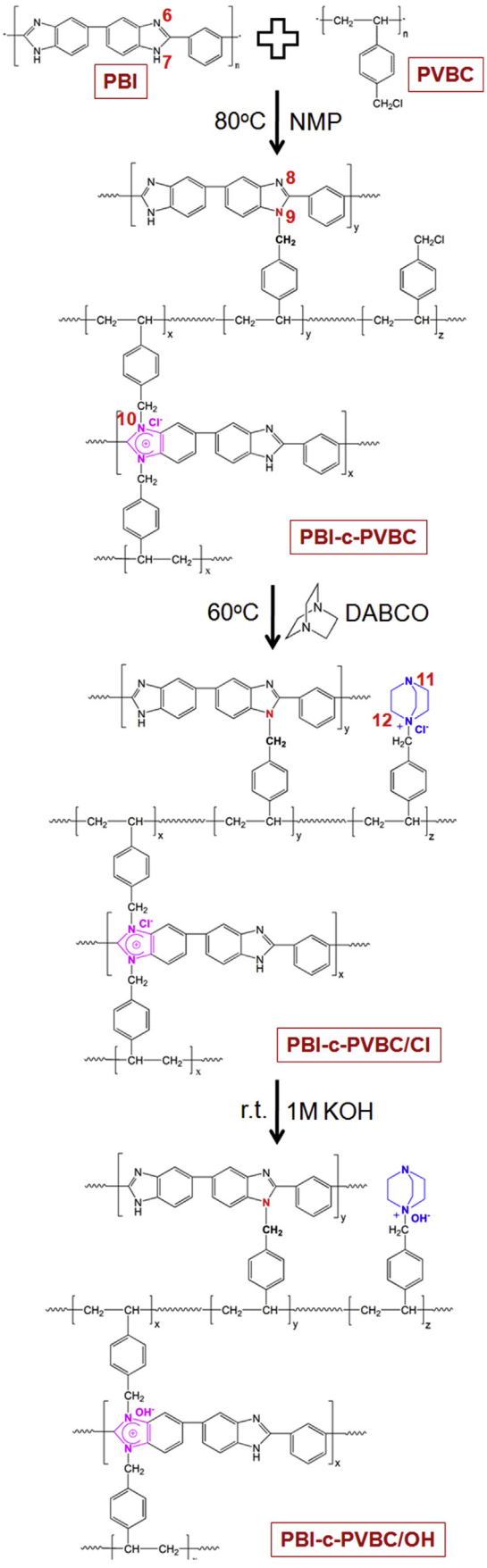

bands just like the combination of PBI and PVBC (Fig. S2), but it was believed that PBI-c-PVBC was not merely the physical mixture of PBI and PVBC, since gelatinization took place after heating the solution of PVBC and PBI at 80 °C for ~5 h, whereas such phenomenon did not occur for pure PBI or PVBC (Fig. S5). Besides, PBI-c-PVBC also showed good solvent-resistance in NMP, while pure PVBC or PBI was easily dissolved in this solvent (Fig. 2). These results suggested crosslinking probably formed between PBI and PVBC.

Based on the molecular structure of PBI and PVBC, the crosslinking was probably formed *via* the N-alkylation of benzimidazole moieties by $-CH_2Cl$ groups. Recently, Yang et al. [33] and Zhang et al. [34] found that an S_N2 type reaction could occur between $-CH_2Cl$ group of PVBC and amine group (−NH−) of PBI at elevated temperature without the use of highly flammable hydride (*e.g.*, LiH and NaH). However, they did not mention whether the other N containing group, imine (=N−), will react with $-CH_2Cl$ group. Note that, it was reported that the imine group in the imidazole ring (*e.g.*, 1-methylimidazole) could react with $-CH_2Cl$ group to form imidazolium salts [35,36], and the reaction between imine groups in a polymer (PBI) and alkylhalides (C_2H_5Br) has also been reported [37]. Hence, we assumed that the imine of PBI could also reacted with $-CH_2Cl$ group of PVBC. In order to verify the reaction product, a model reaction was conducted by use of benzimidazole and benzyl chloride under similar conditions with that in the preparation of PBI-c-PVBC. The model reaction results demonstrated the reaction of amine and imine in imidazole ring with $-CH_2Cl$ groups under heating conditions in NMP (Fig. S6 and S7). As a result, PBI and PVBC will react through the N-alkylation of benzimidazole with $-CH_2Cl$ groups of PVBC, giving rise to crosslinked PBI-c-PVBC membrane with two kinds of crosslinking point: non-conductive point (alkylated amine) [33] and conductive point (benzimidazolium). XPS was adopted to distinguish different N species in the compound and polymer (Fig. 3 and Table S1). As for BIm (Fig. 3a), the peak at 398.7 eV and 400.0 eV was attributed to the nitrogen of imine (=N−) and amine (−NH−), respectively [38]. After reaction, the H atom in −NH− of BIm was replaced by a carbon atom, giving rise to benzyl benzimidazole (BBIm), in which both the binding energy of nitrogen in tertiary amine (R_3N) and imine presented a slight increase in comparison to BIm (Fig. 3b) [34]. The N 1s signal of the other model reaction product, dibenzyl benzimidazolium chloride (DBBImCl), should appear in an even higher binding energy due to the positive charge of imidazolium (Fig. 3b) [38]. As for the polymer, the N 1s peak positions of PBI (Fig. 3c) were in line with BIm and literature [39]. The positions of the crosslinking point were determined according to BBIm and DBBImCl, and the spectrum was presented in Fig. 3d.

For the sake of further proving the crosslinking between PBI and PVBC, the thermogravimetric (TG) analysis was carried out. As shown in Fig. 4a, PBI is thermal stable up to ~600 °C [31]; PVBC starts to degrade from ~350 °C, which comes from the degradation of $-CH_2Cl$ groups, and then the decomposition of main chain occurs above 450 °C. As for PBI-c-PVBC, the weight loss before 150 °C may result from the release of residual solvent, which is followed by a new weight loss step, probably due to the degradation of conductive crosslinking point (benzimidazolium) formed between PBI and $-CH_2Cl$ groups, and thereafter the weight loss may come from the decomposition of the non-conductive crosslinking points and remaining $-CH_2Cl$ groups in PVBC. Therefore, it can be seen that the TG curve of PBI-c-PVBC is totally different from that of PBI and PVBC, *i.e.*, PBI-c-PVBC was not the simple physical mixture of PBI

Fig. 1. Preparation pathway of PBI-c-PVBC/OH membrane. The different nitrogen atom is marked by Arabic numeral and the corresponding N 1s spectrum is displayed in Fig. 3.

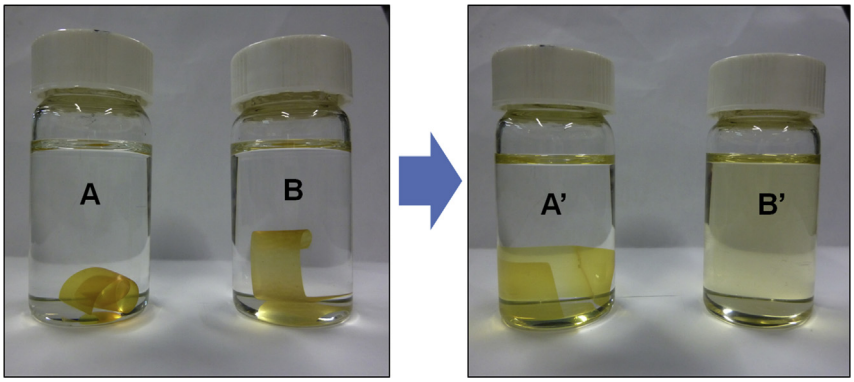

Fig. 2. Photographs of PBI-c-PVBC (A and A′) and PBI (B and B′) before and after immersing in NMP for 72 h. Note that the color of B′ was faint yellow instead of colorless due to the low concentration of PBI. (For interpretation of the references to colour in this figure legend, the reader is referred to the web version of this article.)

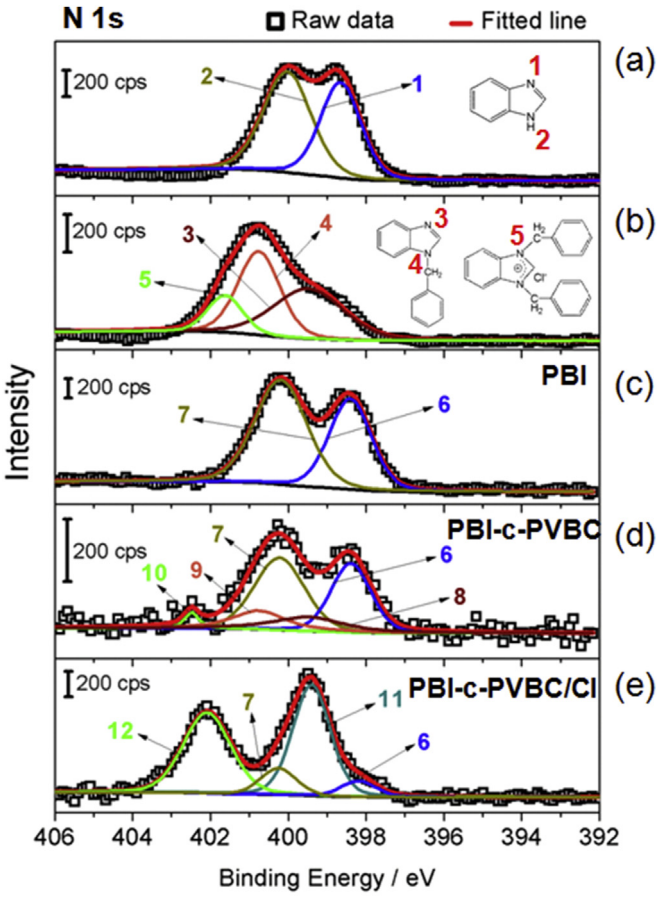

Fig. 3. XPS spectra (N 1s) for (a) benzimidazole (BIm), (b) mixture of benzyl benzimidazole (BBIm) and dibenzyl benzimidazolium chloride (DBBImCl), (c) PBI, (d) PBI-c-PVBC and (e) PBI-c-PVBC/Cl; the peak marked by Arabic numeral corresponds to N atom denoted with the same number shown in Fig. 3 or Fig. 1. Note that some small peaks are not presented in (e) for clarity.

and PVBC.

On the basis of the above results (model reaction, XPS and TG), crosslinking between PBI and PVBC in PBI-c-PVBC was definitely confirmed. The proportion of benzimidazole moieties reacted was estimated to be 34.0% from XPS data (Eqs. S1 and S2) and the corresponding value for PVBC was 37.1% (Eq. S(3)). Due to the crosslinking, the membrane could not dissolve even in its good solvent, and the gel fraction can be measured to estimate the crosslinking density [9,31,40]. As displayed in Fig. 4b, the mass of PBI-c-PVBC membrane does not reduce any more after treatment in NMP for 2 h at 80 °C, and the gel fraction was calculated to be 94.5%, indicating high crosslinking density in the membrane. The crystallinity of various membranes was examined by XRD in a wide range of 2θ degrees (Fig. 4c). The PBI polymer showed a broad peak centered at $2\theta = 26°$ which may arise from a convolution of crystalline and amorphous scattering [41], while PVBC presented two peaks centered at 9° and 21° with higher intensities than PBI, suggesting a higher crystallinity. Interestingly, it is found that the diffraction peaks of PBI-c-PVBC membrane are enhanced significantly with different peak positions from that of PBI and PVBC. This implied that the crosslinking between PBI and PVBC resulted in a new crystalline region [42], which was another evidence for the tight combination between PVBC and PBI.

3.2. Structure analysis of PBI-c-PVBC/OH membrane

After treated with DABCO solutions, remaining -CH_2Cl groups in PBI-c-PVBC were converted to quaternary ammonium (QA) groups, resulting in PBI-c-PVBC/Cl membrane, which was finally transformed to PBI-c-PVBC/OH by alkalization with KOH (Fig. 1). The sufficient conversion of -CH_2Cl groups in PBI-c-PVBC/Cl can be proved by FT-IR and elemental analysis: 1) the absorption band at 1265 cm^{-1} which arises from -CH_2Cl groups [43] disappears in the FT-IR spectrum of PBI-c-PVBC/OH (Fig. S2); 2) only a tiny signal of chlorine element is detected on PBI-c-PVBC/OH compared with PBI-c-PVBC (Fig. 5a and b). Additionally, the thermal stability of PBI-c-PVBC/OH was evaluated by TG. As shown in Fig. 4a, the weight loss before 100 °C comes from the elimination of bonded water of ion exchange groups; the weight loss step starting from ~150 °C may result from the decomposition of QA groups, and similar degradation temperature has been reported on QA groups formed by DABCO [27,44]; above 300 °C, the degradation of side chain and backbone of PVBC can be observed.

As for the membrane with two or more components, such as semi-IPN, blend and composite membranes, the apparent separation of different polymers would occur, which is believed to be adverse to the ionic conductivity or mechanical properties of the polymer electrolyte membrane. In this work, apparent component separation was not observed in the PBI-c-PVBC and/or PBI-c-PVBC/OH membrane: 1) the PBI-c-PVBC membrane presented a transparent and homogeneous appearance (Fig. S4); 2) a uniform distribution of chlorine and nitrogen element was detected across the thickness direction of the membrane (Fig. 5c–f); 3) in the surface and cross-sectional SEM images (Fig. 5g and h), the PBI-c-PVBC/OH membrane showed a uniform and homogeneous morphology,

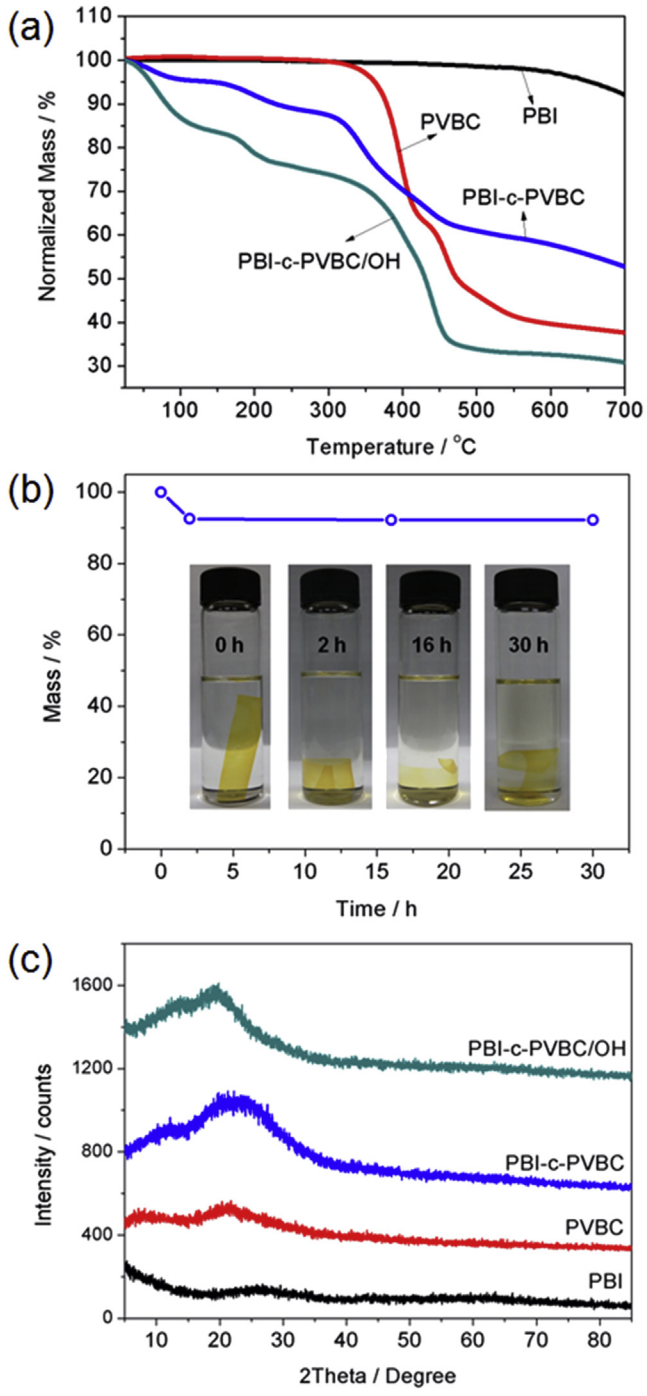

Fig. 4. (a) TG curves for different polymers under N_2 atmosphere; (b) Mass change of PBI-c-PVBC membrane in NMP at 80 °C, and the photos show the PBI-c-PVBC&NMP after different time; (c) XRD patterns for different membranes.

whereas obvious component separation (if any) can be observed in semi-IPN membranes or blend membranes by SEM [18,19,45]. It is believed that crosslinking was an essential factor in the formation of membrane with homogeneity, because lack of interaction between two polymers will cause phase separation, even severe non-uniformity, as shown in our controlled experiments (Fig. S8) and semi-IPN membranes reported previously [18,19].

3.3. Performance evaluation of PBI-c-PVBC/OH membrane

The Cl^-, HCO_3^- and OH^- conductivity of quaternized PBI-c-PVBC at room temperature was 12.1, 12.7 and 25.4 mS cm^{-1}, respectively (Fig. S9). It has been reported that PBI could absorb alkali and showed high OH^- conductivity, but we found that the KOH absorbed by PBI was easily removed during immersing in water, thus the conductance of PBI-c-PVBC/OH was only provided by the QA group formed between DABCO and PVBC (Table S2 and Fig. S10), so there was no electrolyte loss problem for PBI-c-PVBC/OH. The activation energy (E_a) for the transport of OH^- in PBI-c-PVBC/OH was estimated on the basis of Arrhenius plot between conductivity and temperature (Fig. 6a). The calculated E_a for PBI-c-PVBC/OH was 5.5 kJ mol^{-1}, which is smaller than that of AEM usually reported in the literature (8–30 kJ mol^{-1}) [13,46–49], indicating the low resistance of OH^- transport in the membrane probably due to the side-chain-type ionic transport group (quaternized DABCO) and conductive main-chain backbone (conductive crosslinking point in PBI) [46,48].

Despite of such high hydroxide conductivity, the swelling degree and water uptake of PBI-c-PVBC/OH was only ~13% and ~67%, respectively, and they nearly did not grow with the increase of temperature (Fig. 6b), which meant that the excess swelling of AEM by water was inhibited with the aid of crosslinking. Besides, PBI-c-PVBC/OH also presented acceptable toughness (Fig. 6c): the tensile strength and elongation at break of dry PBI-c-PVBC/OH membrane is 17.5 MPa and 8.8%, respectively, while the water-saturated membrane still demonstrated a tensile strength of 7.5 MPa and elongation at break of 11.6%, respectively. In comparison, we found that the quaternized pure PVBC was extremely hydrophilic, even dissolving in the DABCO solution during quaternization (see below); and the crosslinked PVBC membrane fabricated by a micromolecular crosslinker (diethylamine or N, N, N', N′-tetramethyl-1, 6-hexanediamine, not shown) was quite brittle or collapsed after quaternization; and the poly(vinyl acetal) crosslinked PVBC reported in our previous work [29] was also very soft at water-saturated state. As a result, it was considered that both crosslinking and PBI played important roles in fabricating the PBI-c-PVBC/OH membrane: crosslinking improved the interaction between hydrophilic quaternized-PVBC molecules and strong PBI matrix, while PBI strengthened the quaternized-PVBC and supported the whole membrane. Hence, one can see that high dimensional stability, high ionic conductivity and favorable mechanical properties can be achieved simultaneously on AEMs by applying the synthesis strategy here.

We compared the performances of PBI-c-PVBC/OH membrane with other recent-reported semi-IPN and composite AEMs in Table 1. It can be found that the PBI-c-PVBC/OH membrane generally shows lower swelling ratio and water uptake than that of semi-IPNs and composite membranes under similar ionic conductivities no matter what cationic head group is used. However, it should also be pointed out that more water is required to transport hydroxide for PBI-c-PVBC/OH compared with phase-segregated AEMs, probably because PBI-c-PVBC/OH lacks of hydrophilic/hydrophobic phase separation micro-structure, resulting in a lower utilization of water in hydroxide transportation. Therefore, optimizing the structure of ionic conducting channel in the multi-component membrane will be the next task for us.

The PBI-c-PVBC/OH membrane demonstrated striking long-term stability in high alkaline environment. As shown in Fig. 6d, no obvious loss of OH^- conductivity occurred by soaking the membrane in 1 mol L^{-1} KOH at 60 °C for 528 h. Moreover, little change was observed for IEC, swelling ratio and water uptake after this test (Fig. 6e). The tensile strength and elongation at break before and after 528 h was also very close with each other (Fig. 6c).

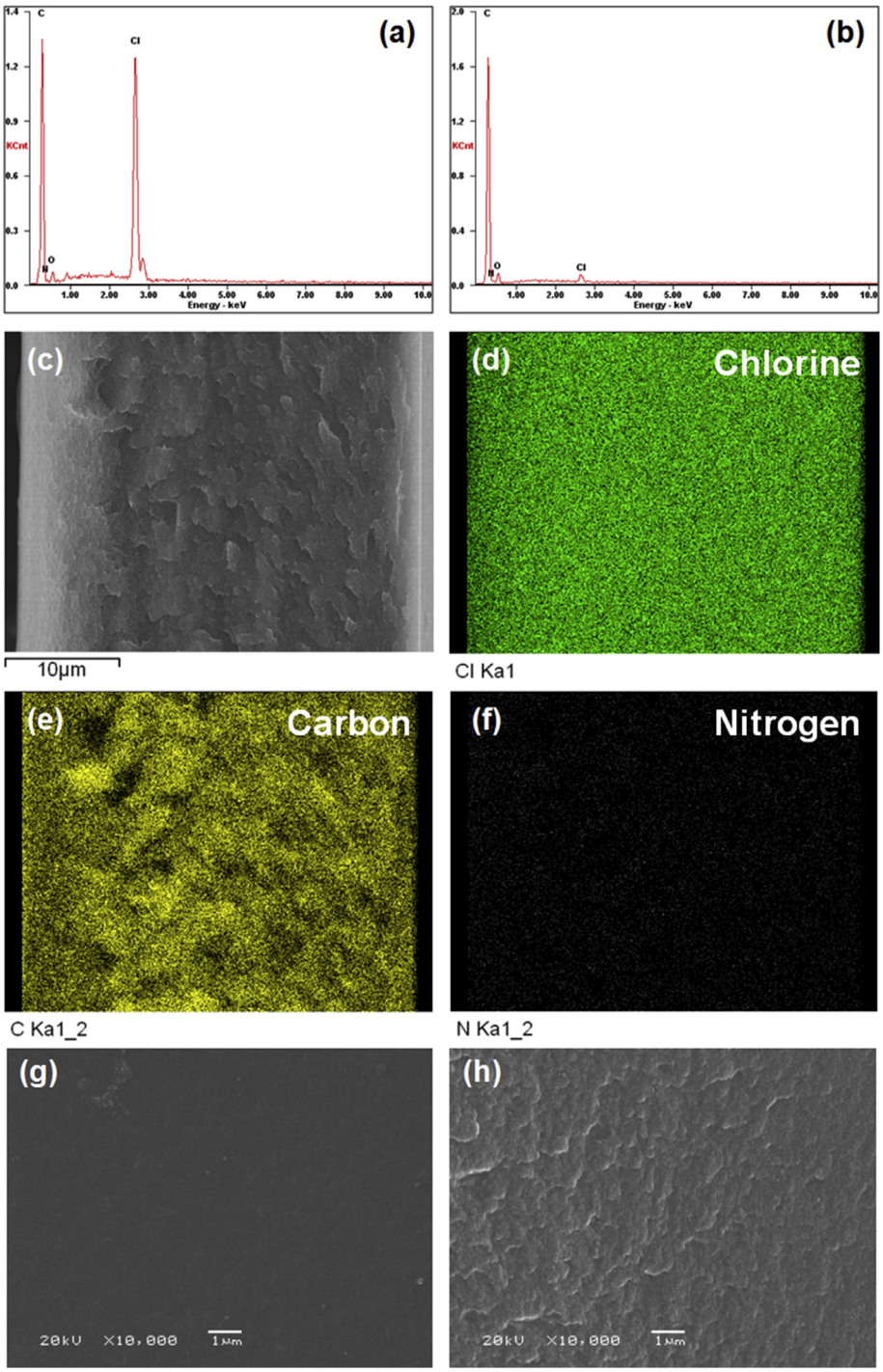

Fig. 5. EDX spectra of (a) PBI-c-PVBC and (b) PBI-c-PVBC/OH; (c–f) The cross-sectional elements distribution of PBI-c-PVBC membrane; (g) Surface and (h) cross-sectional SEM images of PBI-c-PVBC/OH.

Such exceptional qualities should be ascribed to the specific structure of the PBI-c-PVBC/OH. Firstly, the backbone of PBI and PVBC had high alkaline resistance; it was not aromatic-ether structure which was commonly used in AEMs but has been found to be less stable in alkaline environment [20,51]. Secondly, the crosslinking between PBI and PVBC produced a tight-binding structure, which seemed to have enough durability in the strong alkaline environment. Finally, only one, instead of two, tertiary amine in the DABCO molecule was transformed to QA. Although having β-hydrogen atoms, this QA group was supposed to be resistant against Hofmann Elimination owing to its rigidity in structure: the anti-periplanar conformation required for the facile occurrence of Hofmann Elimination was forbidden [2,3]. Moreover, the substitution of DABCO-formed QA by OH^- was slowed down because the acidity of the group and the effect of the nitrogen with positive charge confronting OH^- were reduced due to the other nitrogen atom of DABCO locating in the para-position [2]. Previously, it was difficult to produce DABCO-quaternized AEM with

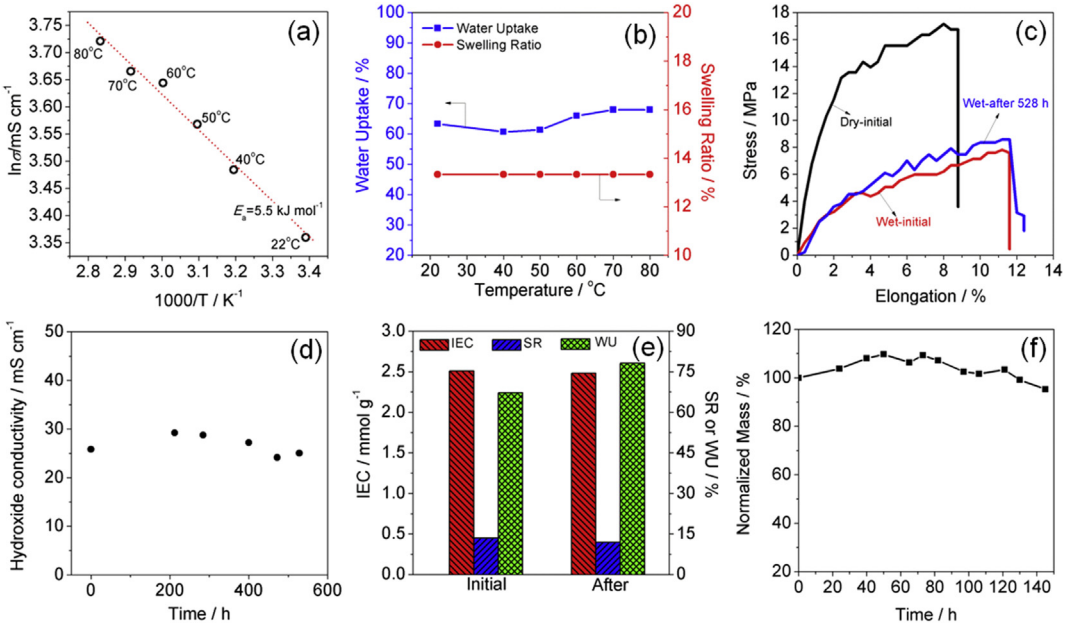

Fig. 6. (a) Hydroxide conductivity at different temperature; (b) Swelling ratio and water uptake of PBI-c-PVBC/OH at different temperature; (c) Stress versus strain curves for the PBI-c-PVBC/OH membrane before and after durability testing in 1 mol L^{-1} KOH for 528 h at 60 °C; (d) Variation of hydroxide conductivity of PBI-c-PVBC/OH at room temperature during immersion in 1 mol L^{-1} KOH at 60 °C; (e) IEC, WU and SR before and after durability testing in 1 mol L^{-1} KOH for 528 h at 60 °C; (f) Mass loss of PBI-c-PVBC/OH membrane in Fenton's reagent at 40 °C.

Table 1
IEC, swelling ratio, water uptake and hydroxide conductivity of PBI-c-PVBC/OH membrane in this work and other AEMs in literature.

Membrane	Membrane type	Ionic group	IEC (mmol g^{-1})	SR (%)	WU (%)	σ (mS cm^{-1})
PBI-c-PVBC/OH (this work)	Crosslinked with macromolecules	DABCO	2.51	13.5 (r.t.[b])	67.2 (r.t.)	25.7 (r.t.)
PVAc(1)-c-PVBC(1)/OH [29]	Crosslinked with macromolecules	imidazolium	1.26	26.3 (r.t.)	139.1 (r.t.)	29 (r.t.)
QPMV-PDVB [17]	Semi-IPN	QATMA[a]	1.19	58 (r.t.)	63.1 (r.t.)	<10 (r.t.)
poly(VBC-co-DVB) [18]	Semi-IPN	QATMA	~1.94	n.a.	90 (r.t.)	15 (r.t.)
QPPT-20 [19]	Semi-IPN	QATMA	~2.31	n.a.	~82 (r.t.)	24 (r.t.)
CQPECH/PTFE/OH$^-$ [15]	Composite	imidazolium	1.64	23.8 (30 °C)	75.8 (30 °C)	15.7 (30 °C)
PTFE-QDPSU [49]	Composite	DABCO	n.a.	17 ± 2	61 ± 3	~26 (~16 °C)
ACD96 [14]	Composite	QATMA	1.54	45 (30 °C)[c]	59.8 (30 °C)	30 (30 °C)
PVBC-b-PS/PPO [50]	Blend&Phase-segregated	QATMA	1.02	n.a.	~31	23
*a*QAPS-S8 [11]	Phase-segregated	QATMA	~1.0	~8 (30 °C)	n.a.	~30 (30 °C)

[a] QATMA = trimethylamine-based quaternary ammonium.
[b] r. t. = room temperature.
[c] The swelling of ACD96 membrane in-plane direction was very small (~3%) due to the rigidity of porous polyethylene substrate, so the swelling ratio in the thickness direction was given, and the corresponding swelling ratio of PBI-c-PVBC/OH was 36.0%.

only one nitrogen of the DABCO molecule reacted, because both of the two nitrogen atoms tended to react, which would give rise to materials with low alkali stabilities [3]. In this work, the "selective conversion" was realized by a post-quaternization method. As shown in the XPS spectrum (Fig. 3e) of PBI-c-PVBC/Cl, the peak at 402.1 eV mainly comes from the N atom marked **12** (Fig. 1) in the QA formed by DABCO and -CH_2Cl (the intensity of the N atom marked **10** was very low), and the peak at 399.4 eV can only be attributed to the N atom in the unreacted tertiary amine of DABCO (marked **11** in Fig. 1) [6,52]. Furthermore, the area ratio of the above two peaks was 48:52, close to 1:1, which confirmed that only one N atom in the DABCO was reacted (a trace amount of crosslinking on DABCO cannot be excluded). That is, XPS technique gave us a direct proof that only one nitrogen in DABCO was converted. Although previous researchers have mentioned that low crosslinking ratio presented in their DABCO-quaternized membranes [43,49], definite evidence was always lacked. It was speculated that every -CH_2Cl group was surrounded by many DABCO molecules during quaternization, thus it was easy for DABCO to react with -CH_2Cl group, leading to the difficulty in forming crosslinking structure (Fig. 7) [53]. Additionally, we found that pure PVBC was dissolved during quaternization by DABCO (Fig. S11), further implying that little crosslinking was produced. This post-quaternization method successfully avoided the crosslinking of DABCO usually encountered when DABCO was added to the halomethylated polymer solution before solvent drying [25,26], thus an alkaline resistant QA group can be produced.

Furthermore, the mass loss of PBI-c-PVBC/OH membrane in Fenton's reagent was monitored to assess the oxidative stability of the membrane. As displayed in Fig. 6f, the mass of the wet membrane increased slowly in the first few hours and then gradually declined, but the membrane did not collapse even after soaking in Fenton's reagent for more than 140 h, which indicated an acceptable durability of PBI-c-PVBC/OH against oxidation. The IEC of PBI-c-PVBC/OH membrane after testing was reduced from 2.51 to 1.79 mmol g^{-1}, suggesting the decomposition of anion exchange groups caused by Fenton's reagent. Moreover, the color of the membrane got darker gradually from faint yellow to brown, and the

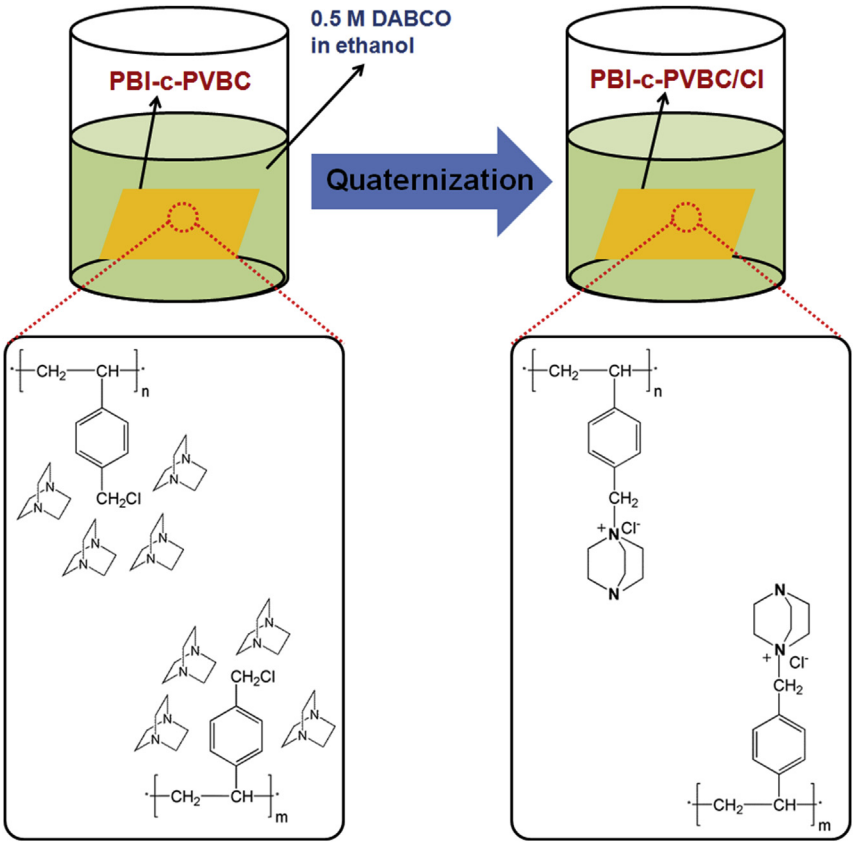

Fig. 7. Scheme of the quaternization of residual -CH_2Cl groups in PBI-c-PVBC membrane. Only one nitrogen of the DABCO reagent was reacted.

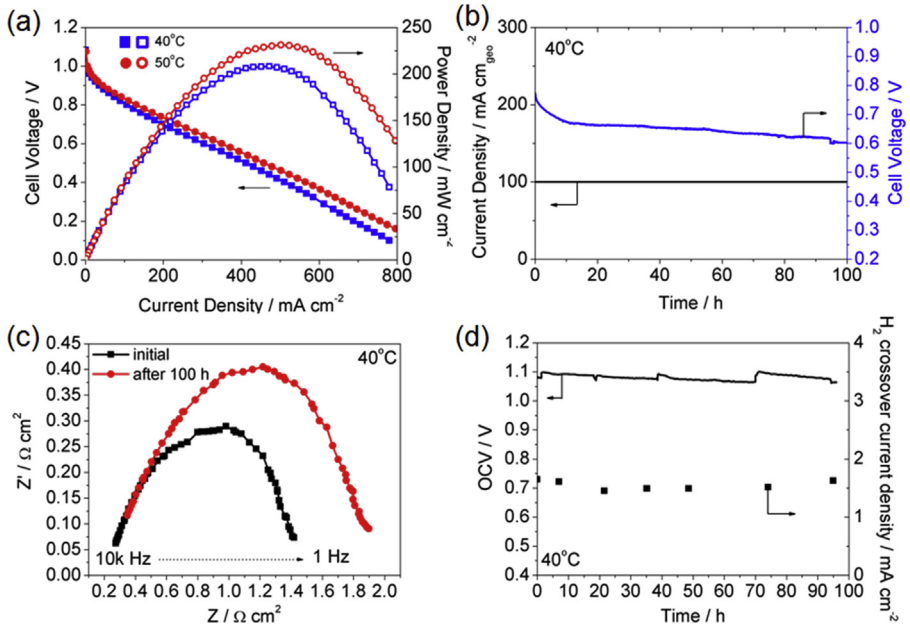

Fig. 8. (a) Polarization curves and power density curves of H_2/O_2 fuel cell with PBI-c-PVBC/OH membrane; (b) Durability test of the fuel cell at 40 °C under constant current density (100 mA cm^{-2}); (c) EIS spectra of fuel cell before and after constant current durability testing; (d) Open circuit voltage (OCV) and H_2 crossover current density of the fuel cell under continuous OCV conditions using fully humidified H_2/O_2 at 40 °C.

membrane became soft and weak after stability test, which implied degradation of the polymer backbone of PBI-c-PVBC/OH. According to the study of proton exchange membrane, the aromatic and hydrocarbon backbone of PBI-c-PVBC/OH may be broken under the attack of radical and then oxidized to carbonyl group [54], which increased the hydrophilicity of the membrane and then caused the

mass increase of AEM in the first few hours. In addition, the unreacted end groups of PBI may also cause degradation of membrane in the oxidative environment [54].

3.4. Fuel cell testing

The single fuel cell testing of PBI-c-PVBC/OH membrane was performed by using H_2/O_2 at 100% humidity and 0.15 MPa (absolute pressure). Based on the literature, the working temperature of AEMFCs was often settled below 50 °C [15,55,56]; thus the polarization curves of fuel cell in this work were recorded at 40 and 50 °C. As shown in Fig. 8a, the open circuit voltage (OCV) of the fuel cell is ~1.07 V, which suggests that PBI-c-PVBC/OH has good gas barrier ability. A peak power density (P_{max}) of 208 mW cm^{-2} and 230 mW cm^{-2} was obtained on the fuel cell at 40 °C and 50 °C, respectively, which was larger than the P_{max} of 145 mW cm^{-2} [57] and 174 mW cm^{-2} [56] presented by an AEMFC applying quaternized polysulfone and A201 (Tokuyama Co., Japan) membrane, respectively, and the electrodes used were all fabricated by AS-4 ionomer and Pt/C catalysts, the same as those used in this work. The remarkable power output ability of AEMFC using PBI-c-PVBC/OH membrane was a strong evidence for the outstanding performances of PBI-c-PVBC/OH. It needs to be pointed out that the performance of AEMFC could be further improved by optimizing the architecture of electrode, operating conditions of fuel cell and so on, but it is beyond the scope of this paper.

The durability of PBI-c-PVBC/OH was also evaluated in the single AEMFC. As demonstrated in Fig. 8b, the fuel cell was performed under constant current of 100 mA cm^{-2}, meanwhile the cell voltage was monitored. It was found that the voltage declined slowly from ~0.7 V to ~0.6 V during the test time of 100 h. The EIS spectrum of fuel cell was recorded in order to analyze the reason of degradation (Fig. 8c). It was found that the EIS spectra at high frequency nearly overlapped before and after testing, indicating little increase of the inner resistance of fuel cell (consisting of membrane resistance). In contrast, the impedance at low frequency, reflecting the electron transfer resistance at electrode, increased from 0.7002 Ω cm^2 to 1.1918 Ω cm^2 (Fig. S12 and Table S3), suggesting that the catalytic performance of the electrode was degraded. The results above revealed that the degradation of fuel cell probably arose from the deterioration of electrode, while the membrane had superior chemical stability, which was consistent with the results of *ex-situ* characterizations. Furthermore, the oxidative stability of PBI-c-PVBC/OH was evaluated under continuous OCV conditions [58]. In the testing period (~100 h), the OCV of the fuel cell was always above 1.06 V and the hydrogen crossover current of AEM did not grow as well (Fig. 8d), indicating that PBI-c-PVBC/OH membrane had good tolerance to oxidative environments.

4. Conclusions

A novel AEM was developed by using PBI and DABCO as the macromolecular crosslinker and quaternization reagent for PVBC, respectively. The PBI-c-PVBC/OH membrane exhibited good flexibility, high conductivity and superior dimensional and chemical stability simultaneously. Optimization of the structure of PBI and ionic conductive component would further improve the performance of AEM. The strategy reported here should be regarded as a methodological improvement in the development of AEM and could be used to fabricate other membrane materials.

Acknowledgments

This work was financially supported by the National High Technology Research and Development Program of China (863 Program, No. 2013AA110201), National Basic Research Program of China (973 Program, No. 2012CB215500) and the National Natural Science Foundations of China (No. 21306190).

Appendix A. Supplementary data

Supplementary data related to this article can be found at http://dx.doi.org/10.1016/j.jpowsour.2015.07.048.

References

[1] Y.-J. Wang, J. Qiao, R. Baker, J. Zhang, Alkaline polymer electrolyte membranes for fuel cell applications, Chem. Soc. Rev. 42 (2013) 5768–5787.
[2] G. Couture, A. Alaaeddine, F. Boschet, B. Ameduri, Polymeric materials as anion-exchange membranes for alkaline fuel cells, Prog. Polym. Sci. 36 (2011) 1521–1557.
[3] J.R. Varcoe, P. Atanassov, D.R. Dekel, A.M. Herring, M.A. Hickner, P.A. Kohl, A.R. Kucernak, W.E. Mustain, K. Nijmeijer, K. Scott, T.W. Xu, L. Zhuang, Anion-exchange membranes in electrochemical energy systems, Energy Environ. Sci. 7 (2014) 3135–3191.
[4] G. Merle, M. Wessling, K. Nijmeijer, Anion exchange membranes for alkaline fuel cells: a review, J. Membr. Sci. 377 (2011) 1–35.
[5] J. Pan, C. Chen, L. Zhuang, J.T. Lu, Designing advanced alkaline polymer electrolytes for fuel cell applications, Acc. Chem. Res. 45 (2012) 473–481.
[6] J. Pan, Y. Li, L. Zhuang, J. Lu, Self-crosslinked alkaline polymer electrolyte exceptionally stable at 90 °C, Chem. Commun. 46 (2010) 8597–8599.
[7] L. Wang, M.A. Hickner, Low-temperature crosslinking of anion exchange membranes, Polym. Chem. 5 (2014) 2928–2935.
[8] N. Li, L. Wang, M. Hickner, Cross-linked comb-shaped anion exchange membranes with high base stability, Chem. Commun. 50 (2014) 4092–4095.
[9] A.H.N. Rao, S. Nam, T.-H. Kim, Crosslinked poly(arylene ether sulfone) block copolymers containing pendant imidazolium groups as both crosslinkage sites and hydroxide conductors for highly selective and stable membranes, Int. J. Hydrogen Energy 39 (2014) 5919–5930.
[10] N. Li, T. Yan, Z. Li, T. Thurn-Albrecht, W.H. Binder, Comb-shaped polymers to enhance hydroxide transport in anion exchange membranes, Energy Environ. Sci. 5 (2012) 7888–7892.
[11] J. Pan, C. Chen, Y. Li, L. Wang, L. Tan, G. Li, X. Tang, L. Xiao, J. Lu, L. Zhuang, Constructing ionic highway in alkaline polymer electrolytes, Energy Environ. Sci. 7 (2014) 354–360.
[12] M. Tanaka, K. Fukasawa, E. Nishino, S. Yamaguchi, K. Yamada, H. Tanaka, B. Bae, K. Miyatake, M. Watanabe, Anion conductive block poly(arylene ether)s: synthesis, properties, and application in alkaline fuel cells, J. Am. Chem. Soc. 133 (2011) 10646–10654.
[13] Q. Li, L. Liu, Q. Miao, B. Jin, R. Bai, A novel poly(2,6-dimethyl-1,4-phenylene oxide) with trifunctional ammonium moieties for alkaline anion exchange membranes, Chem. Commun. 50 (2014) 2791–2793.
[14] Y. Zhao, H. Yu, F. Xie, Y. Liu, Z. Shao, B. Yi, High durability and hydroxide ion conducting pore-filled anion exchange membranes for alkaline fuel cell applications, J. Power Sources 269 (2014) 1–6.
[15] J. Hu, D. Wan, W. Zhu, L. Huang, S. Tan, X. Cai, X. Zhang, Fabrication of a high-stability cross-linked quaternized poly(epichlorolydrin)/ptfe composite membrane via a facile route, ACS Appl. Mater. Interfaces 6 (2014) 4720–4730.
[16] J.L. Wang, R.H. He, Q.T. Che, Anion exchange membranes based on semi-interpenetrating polymer network of quaternized chitosan and polystyrene, J. Colloid Interface Sci. 361 (2011) 219–225.
[17] Y. Luo, J. Guo, C. Wang, D. Chu, Fuel cell durability enhancement by cross-linking alkaline anion exchange membrane electrolyte, Electrochem. Commun. 16 (2012) 65–68.
[18] X. Lin, M. Gong, Y. Liu, L. Wu, Y. Li, X. Liang, Q. Li, T. Xu, A convenient, efficient and green route for preparing anion exchange membranes for potential application in alkaline fuel cells, J. Membr. Sci. 425–426 (2013) 190–199.
[19] X. Lin, Y. Liu, S.D. Poynton, A.L. Ong, J.R. Varcoe, L. Wu, Y. Li, X. Liang, Q. Li, T. Xu, Cross-linked anion exchange membranes for alkaline fuel cells synthesized using a solvent free strategy, J. Power Sources 233 (2013) 259–268.
[20] C. Fujimoto, D.-S. Kim, M. Hibbs, D. Wrobleski, Y.S. Kim, Backbone stability of quaternized polyaromatics for alkaline membrane fuel cells, J. Membr. Sci. 423–424 (2012) 438–449.
[21] Z. Si, L. Qiu, H. Dong, F. Gu, Y. Li, F. Yan, Effects of substituents and substitution positions on alkaline stability of imidazolium cations and their corresponding anion-exchange membranes, ACS Appl. Mater. Interfaces 6 (2014) 4346–4355.
[22] Y. Zha, M.L. Disabb-Miller, Zachary D. Johnson, M.A. Hickner, G.N. Tew, Metal-cation-based anion exchange membranes, J. Am. Chem. Soc. 134 (2012) 4493–4496.
[23] F.L. Gu, H.L. Dong, Y.Y. Li, Z. Sun, F. Yan, Base stable pyrrolidinium cations for alkaline anion exchange membrane applications, Macromolecules 47 (2014) 6740–6747.
[24] J. Si, S. Lu, X. Xu, S. Peng, R. Xiu, Y. Xiang, A gemini quaternary ammonium poly (ether ether ketone) anion-exchange membrane for alkaline fuel cell: design, synthesis, and properties, ChemSusChem 7 (2014) 3389–3395.

[25] A. Katzfuss, V. Gogel, L. Jorissen, J. Kerres, The application of covalently cross-linked BrPPO as AEM in alkaline DMFC, J. Membr. Sci. 425 (2013) 131–140.
[26] E. Guler, Y.L. Zhang, M. Saakes, K. Nijmeijer, Tailor-made anion-exchange membranes for salinity gradient power generation using reverse electrodialysis, ChemSusChem 5 (2012) 2262–2270.
[27] J. Fang, Y. Yang, X. Lu, M. Ye, W. Li, Y. Zhang, Cross-linked, ETFE-derived and radiation grafted membranes for anion exchange membrane fuel cell applications, Int. J. Hydrogen Energy 37 (2012) 594–602.
[28] C. Sollogoub, A. Guinault, C. Bonnebat, M. Bennjima, L. Akrour, J.F. Fauvarque, L. Ogier, Formation and characterization of crosslinked membranes for alkaline fuel cells, J. Membr. Sci. 335 (2009) 37–42.
[29] W. Lu, Z.-G. Shao, G. Zhang, Y. Zhao, B. Yi, Crosslinked poly(vinylbenzyl chloride) with a macromolecular crosslinker for anion exchange membrane fuel cells, J. Power Sources 248 (2014) 905–914.
[30] Q.A. Zhang, S.H. Li, S.B. Zhang, A novel guanidinium grafted poly(aryl ether sulfone) for high-performance hydroxide exchange membranes, Chem. Commun. 46 (2010) 7495–7497.
[31] Y.S. Guan, H.T. Pu, M. Jin, Z.H. Chang, D.C. Wan, Preparation and characterisation of proton exchange membranes based on crosslinked polybenzimidazole and phosphoric acid, Fuel Cells 10 (2010) 973–982.
[32] H.A. Gasteiger, S.S. Kocha, B. Sompalli, F.T. Wagner, Activity benchmarks and requirements for Pt, Pt-alloy, and non-Pt oxygen reduction catalysts for PEMFCs, Appl. Catal. B 56 (2005) 9–35.
[33] J.S. Yang, D. Aili, Q.F. Li, L.N. Cleemann, J.O. Jensen, N.J. Bjerrum, R.H. He, Covalently cross-linked sulfone polybenzimidazole membranes with poly(-vinylbenzyl chloride) for fuel cell applications, ChemSusChem 6 (2013) 275–282.
[34] N. Zhang, C.J. Zhao, W.J. Ma, S. Wang, B.L. Wang, G. Zhang, X.F. Li, H. Na, Macromolecular covalently cross-linked quaternary ammonium poly(ether ether ketone) with polybenzimidazole for anhydrous high temperature proton exchange membranes, Polym. Chem. 5 (2014) 4939–4947.
[35] X.M. Yan, G.H. He, S. Gu, X.M. Wu, L.G. Du, Y.D. Wang, Imidazolium-functionalized polysulfone hydroxide exchange membranes for potential applications in alkaline membrane direct alcohol fuel cells, Int. J. Hydrogen Energy 37 (2012) 5216–5224.
[36] X. Lin, X. Liang, S.D. Poynton, J.R. Varcoe, A.L. Ong, J. Ran, Y. Li, Q. Li, T. Xu, Novel alkaline anion exchange membranes containing pendant benzimidazolium groups for alkaline fuel cells, J. Membr. Sci. 443 (2013) 193–200.
[37] H. Hou, S. Wang, H. Liu, L. Sun, W. Jin, M. Jing, L. Jiang, G. Sun, Synthesis and characterization of a new anion exchange membrane by a green and facile route, Int. J. Hydrogen Energy 36 (2011) 11955–11960.
[38] G. Bhargava, T.A. Ramanarayanan, S.L. Bernasek, Imidazole–Fe Interaction in an aqueous chloride medium: effect of cathodic reduction of the native oxide, Langmuir 26 (2009) 215–219.
[39] A.G. Nurioglu, H. Akpinar, F.E. Kanik, D. Toffoli, L. Toppare, Further investigation of intramolecular H-bonding in benzimidazole and EDOT containing monomer, J. Electroanal. Chem. 693 (2013) 23–27.
[40] S. Xu, G. Zhang, Y. Zhang, C. Zhao, L. Zhang, M. Li, J. Wang, N. Zhang, H. Na, Cross-linked hydroxide conductive membranes with side chains for direct methanol fuel cell applications, J. Mater. Chem. 22 (2012) 13295–13302.
[41] P. Staiti, F. Lufrano, A.S. Aricò, E. Passalacqua, V. Antonucci, Sulfonated polybenzimidazole membranes — preparation and physico-chemical characterization, J. Membr. Sci. 188 (2001) 71–78.
[42] A. Mondal, B. Mandal, Synthesis and characterization of crosslinked poly(vinyl alcohol)/poly(allylamine)/2-amino-2-hydroxymethyl-1,3-propanediol/polysulfone composite membrane for CO2/N2 separation, J. Membr. Sci. 446 (2013) 383–394.
[43] M. Faraj, E. Elia, M. Boccia, A. Filpi, A. Pucci, F. Ciardelli, New anion conducting membranes based on functionalized styrene-butadiene-styrene triblock copolymer for fuel cells applications, J. Polym. Sci. Pol. Chem. 49 (2011) 3437–3447.
[44] S. Maurya, S.H. Shin, M.K. Kim, S.H. Yun, S.H. Moon, Stability of composite anion exchange membranes with various functional groups and their performance for energy conversion, J. Membr. Sci. 443 (2013) 28–35.
[45] M.A. Vandiver, B.R. Caire, Z. Poskin, Y.F. Li, S. Seifert, D.M. Knauss, A.M. Herring, M.W. Liberatore, Durability and performance of polystyrene-b-poly(vinylbenzyl trimethylammonium) diblock copolymer and equivalent blend anion exchange membranes, J. Appl. Polym. Sci. 132 (2015), http://dx.doi.org/10.1002/app.41596.
[46] L.-c. Jheng, S.L.-c. Hsu, B.-y. Lin, Y.-l. Hsu, Quaternized polybenzimidazoles with imidazolium cation moieties for anion exchange membrane fuel cells, J. Membr. Sci. 460 (2014) 160–170.
[47] J. Zhang, J. Qiao, G. Jiang, L. Liu, Y. Liu, Cross-linked poly(vinyl alcohol)/poly (diallyldimethylammonium chloride) as anion-exchange membrane for fuel cell applications, J. Power Sources 240 (2013) 359–367.
[48] X. Li, G. Nie, J. Tao, W. Wu, L. Wang, S. Liao, Assessing the influence of side-chain and main-chain aromatic benzyltrimethyl ammonium on anion exchange membranes, ACS Appl. Mater. Interfaces 6 (2014) 7585–7595.
[49] X. Wang, M.Q. Li, B.T. Golding, M. Sadeghi, Y.C. Cao, E.H. Yu, K. Scott, A polytetrafluoroethylene-quaternary 1,4-diazabicyclo- 2.2.2 -octane polysulfone composite membrane for alkaline anion exchange membrane fuel cells, Int. J. Hydrogen Energy 36 (2011) 10022–10026.
[50] Y. Li, A.C. Jackson, F.L. Beyer, D.M. Knauss, Poly(2,6-dimethyl-1,4-phenylene oxide) blended with poly(vinylbenzyl chloride)-b-polystyrene for the formation of anion exchange membranes, Macromolecules 47 (2014) 6757–6767.
[51] C.G. Arges, V. Ramani, Two-dimensional NMR spectroscopy reveals cation-triggered backbone degradation in polysulfone-based anion exchange membranes, Proc. Natl. Acad. Sci. USA 110 (2013) 2490–2495.
[52] R. Zeng, J. Handsel, S.D. Poynton, A.J. Roberts, R.C.T. Slade, H. Herman, D.C. Apperley, J.R. Varcoe, Alkaline ionomer with tuneable water uptakes for electrochemical energy technologies, Energy Environ. Sci. 4 (2011) 4925–4928.
[53] M. Faraj, M. Boccia, H. Miller, F. Martini, S. Borsacchi, M. Geppi, A. Pucci, New LDPE based anion-exchange membranes for alkaline solid polymeric electrolyte water electrolysis, Int. J. Hydrogen Energy 37 (2012) 14992–15002.
[54] D. Zhao, J.H. Li, M.K. Song, B.L. Yi, H.M. Zhang, M.L. Liu, A durable alternative for proton-exchange membranes: sulfonated poly(benzoxazole thioether sulfone)s, Adv. Energy Mater 1 (2011) 203–211.
[55] Z. Zhang, L. Wu, J. Varcoe, C. Li, A.L. Ong, S. Poynton, T. Xu, Aromatic polyelectrolytes via polyacylation of pre-quaternized monomers for alkaline fuel cells, J. Mater. Chem. A 1 (2013) 2595–2601.
[56] K. Matsumoto, T. Fujigaya, H. Yanagi, N. Nakashima, Very high performance alkali anion-exchange membrane fuel cells, Adv. Funct. Mater 21 (2011) 1089–1094.
[57] Y. Zhao, J. Pan, H. Yu, D. Yang, J. Li, L. Zhuang, Z. Shao, B. Yi, Quaternary ammonia polysulfone-PTFE composite alkaline anion exchange membrane for fuel cells application, Int. J. Hydrogen Energy 38 (2013) 1983–1987.
[58] D. Zhao, B.L. Yi, H.M. Zhang, M.L. Liu, The effect of platinum in a Nafion membrane on the durability of the membrane under fuel cell conditions, J. Power Sources 195 (2010) 4606–4612.